2023-03-07

Developable Mechanisms on Right Conical Surfaces

Lance P. Hyatt
Brigham Young University - Provo

Spencer P. Magleby
Brigham Young University - Provo, magleby@byu.edu

Larry L. Howell
Brigham Young University - Provo, lhowell@byu.edu

Original Publication Citation

Hyatt, L.P., Magleby, S.P., Howell, L.L., "Developable Mechanisms on Right Conical Surfaces," Mechanism and Machine Theory, Vol. 149, paper no. 103813, https://doi.org/10.1016/j.mechmachtheory.2020.103813, 2020.

Developable Mechanisms on Right Conical Surfaces

Lance P. Hyatt, Spencer P. Magleby, Larry L. Howell

Brigham Young University
Department of Mechanical Engineering
350 EB, Provo UT 84602

Abstract

An approach for designing developable mechanisms on a conical surface is presented. By aligning the joint axes of spherical mechanisms to the ruling lines, the links can be created in a way that the mechanism conforms to a conical surface. Terminology is defined for mechanisms mapped onto a right cone. Models are developed to describe the motion of the mechanism with respect to the apex of the cone, and connections are made to cylindrical developable mechanisms using projected angles. The Loop Sum Method is presented as an approach to determine the geometry of the cone to which a given spherical mechanism can be mapped. A method for position analysis is presented to determine the location of any point along the link of a mech anism with respect to the conical geometry. These methods are also applied to multiloop spherical mechanisms.

Keywords: Developable mechanism, spherical mechanism, conical surface, compact mechanism

1. Introduction

Developable mechanisms are mechanisms that can conform to a devel opable surface at some point in its motion [1]. Developable surfaces (cylinders, cones, and tangent developable surfaces) are found in many areas including aerospace [2], watercraft design [3], architecture [4, 5], and medical devices [6]. Many aerospace structures have cylindrical bodies and conical noses [7]. If a developable mechanism is placed on either surface, it could be launched in the compact, conformed position and then be deployed later in flight in creasing the potential functionality of the rocket with little cost in volume, similar to the benefits of deployable solar arrays [8]. These same principles

can also be applied at a smaller scale in medical devices where the tools continue to decrease in size [9]. For example, a minimally invasive surgical device needs to enter through a small incision and then a mechanism embedded in the developable shaft could expand increasing the potential function of the device.

Several methods for spherical mechanism design and analysis exist [10, 11, 12, 13, 14, 15], but do not consider the constraints of conforming to a specific surface. The complex motion of these spherical mechanisms have several applications to control the orientation of items in assembly processes [16], multi-DOF wrists [17], parallel mechanisms [18, 19], gripper mechanisms [20], designing rigid origami [21], and medical rehabilitation devices [22]. This paper introduces tools to aid in the design and analysis of mechanisms on right conical surfaces. A background on developable mechanisms is given along with some of the analysis methods for cylindrical developable mechanisms. Some conventions of spherical mechanisms are also presented. Terms and definitions for conical developable mechanisms are then introduced. These definitions facilitate a connection to the design methods for cylindrical developable mechanisms. A method to determine the geometry of a cone to which a spherical mechanism can be mapped is introduced. Finally, an approach for the position analysis of a conical developable mechanism is presented based on the geometry of the conical surface.

2. Background

2.1. Developable Surfaces

Developable surfaces have been studied and utilized in a variety of fields from architecture and engineering to computer science [23, 5]. When restricting our definition to R^3space, developable surfaces are a subset of ruled surfaces, have zero Gaussian curvature, are isometric to a plane, and are an envelope of a 1-parameter family of planes [24, 25]. As a ruled surface, it can be formed by moving a straight line (a ruling line) through space. For a ruled surface to be developable, the ruling line must characterize one of the principle curvatures, causing the product of the principle curvatures (Gaussian curvature) to be zero. Being isometric to a plane means that any distance between two points measured along the surface will remain constant if the surface is flattened onto a plane. A useful description of developable surfaces is any surface that can be flattened to a plane without stretching or tearing.

Figure 1: Three non-trivial developable surfaces: (left) generalized cylinder, (middle) generalized cone, and (right) tangent developable surface.

There are three non-trivial types of developable surfaces apart from a plane: generalized cylinders, generalized cones, and tangent developable surfaces. The ruling lines of a generalized cylinder are all parallel while the ruling lines of a generalized cone all converge to a point. The ruling lines for a tangent developed surface are all tangent to a spacial curve. Figure 1 shows examples of the three types of developable surfaces.

2.2. Developable Mechanisms

Developable mechanisms are defined as mechanisms that fulfill three requirements [1]:

1. Are contained within or conform to developable surfaces when both are modeled with zero-thickness
2. Have mobility
3. Do not require the developable surface to deform to enable the mechanism's movement

These mechanisms are facilitated by aligning revolute joint axes along the ruling lines of the host developable surface. This is known as the Hinge Axis Ruling Condition [1]. By applying this condition to the three non-trivial developable surfaces, different types of mechanisms can be mapped to each surface. Planar mechanisms can be mapped to cylindrical surfaces, spherical mechanisms can be mapped to conical surfaces, and spatial mechanisms can be mapped to tangent developable surfaces. Nelson et al. presents examples

of the three types of mechanisms, while this work focuses on conical devel opable mechanisms [1]. The surface to which a developable mechanism is mapped is called the reference surface.

Traditional kinematic analysis of mechanisms relies only on the relative location of the joints, and the links can have any arbitrary shape [26]. However, to satisfy the first requirement, the links of a developable mechanism must also conform to the reference surface. Greenwood et al. defined this as the link-shape condition [27].

2.3. Spherical Mechanisms

While planar mechanism motion is limited to two dimensions, spherical mechanisms move in three dimensions. They are a subset of spatial mechanisms with all of their joint axes converging to a single point. For this special case, any point on the mechanism will be constrained to motion on a reference sphere around the point where the axes converge.

Planar mechanisms appear as a limiting case of spherical

mechanisms with a center point at infinity [28]. While planar mechanism kinematics are determined by link lengths, the kinematics of spherical mechanisms are defined by the link angles [13]. The loop equations used to analyze spherical mechanisms are typically compositions of rotations about a base frame located at the point where the axes converge rather than vector loops of complex numbers commonly used for planar mechanisms. These differences require special consideration as some analysis techniques for planar mechanisms may not apply to spherical mechanisms [12].

Traditional spherical mechanisms are represented with links that conform to a reference sphere on which they travel. Figure 2 is an example of a spherical four-bar mechanism with the link angles labeled. While several conventions have been used to describe spherical four-bar mechanisms, this paper will use the convention presented by McCarthy [13]. The links α, η, β, and γ refer to the input, coupler, output, and ground link, respectively. A reference coordinate frame is placed with the origin F where the joint axes converge with the z-axis in the direction of O. The y-axis is oriented along the vector O×C. The input angle θ is the angle about O, and the output angle ψ about C, both measured counterclockwise from the xz plane.

A coupler angle ξ is defined as the dihedral angle between planes OFA and AFB.

For any spherical mechanism, there exist a number of supplementary spherical linkages that are kinematically equivalent [12]. This is because the

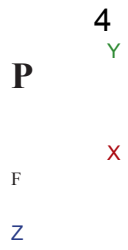

Figure 2: A traditional 4-bar spherical mechanism with all axes and link angles labeled, and the links following the surface of a sphere.

joint axes intersect the center of the reference sphere, and cross the surface of the sphere in two locations. A spherical link is created as a portion of the great circle connecting two different joint axes along the reference sphere. With the two intersecting locations, there are multiple options to connect the joint axes to create mechanisms with different link

angles but identical kinematic behavior. For example, any given four-bar spherical mechanism has 15 other kinematically equivalent configurations if the link angles in each supplementary linkage is no greater than 360°.

Grashof's criterion used for planar four-bar mechanisms can also be applied to spherical four-bar mechanisms [29]. A mechanism is a Grashof mechanism if one of the links can rotate completely relative to the other links.

McCarthy introduced four parameters based on the link angles that can be used to determine the classification of a mechanism [13]. The four parameters T_1, T_2, T_3, and T_4 are defined below.

$$T_1 = \gamma - \alpha + \eta - \beta \quad (1)$$

$$T_2 = \gamma - \alpha - \eta + \beta \quad (2)$$

$$T_3 = \eta + \beta - \gamma - \alpha \quad (3)$$

$$T_4 = 360^\circ - \alpha - \eta - \beta - \gamma \quad (4)$$

When you multiply these parameters together, the sign of the product will indicate whether a mechanism satisfies Grashof's criterion. If the product is positive ($T_1T_2T_3T_4 > 0$), the mechanism will be a Grashof linkage, and a negative product ($T_1T_2T_3T_4 < 0$) defines a nonGrashof linkage. A mechanism is folded if one or more of the parameters listed is zero. This means that at some point in the motion of the linkage, all joint axis can lie on a plane.

2.4. Instant Centers and Instant Pole Axes

In planar kinematics, instant centers are often used for the velocity analy sis of a mechanism [26]. An instant center is a point where there is no relative velocity between two bodies at a given instant [30]. This principle is useful when determining the relative motion of a mechanism in a given configuration. An analog for instant centers exists in spherical mechanisms commonly

referred to as relative or instant pole axes [12, 31]. For two spherical links, α and η, the instant pole axis is denoted as $P_{\alpha\eta}$. This is the axis about which each link rotates relative to each other. The points where this axis intersects the reference sphere are points where there is no relative velocity between the two links.

For a spherical mechanism, the instant pole axis of two adjacent links is the joint axis that connects them. For the mechanism shown in Fig. 2 the instant pole axis $P_{\alpha\eta}$ is joint axis A. For the links on opposite sides of the mechanism, the instant pole axis can be determined by extending two great circles that contain the other two links and finding their intersection on the

reference sphere. The instant pole axis is the line that passes through that

intersection and the center of the reference sphere. To find the instant pole axis $P_{\eta\gamma}$ of the mechanism in Fig. 2, a great circle that passes through *O* and *A* intersects with a great circle that passes through *C* and *B* at point *P*. The instant pole axis passes through point *P* and the center of the reference sphere as shown in Fig. 3.

Figure 3: The instant pole axis $P_{\eta\gamma}$ which represents the axis about which link η rotates with respect to link γ.

2.5. Intramobility, Extramobility, and Transmobility

A developable mechanism is defined as conforming to or being contained within a developable surface, so it is helpful to understand the motion of the mechanism relative to the reference surface. Three classifications for developable mechanisms have been defined by Greenwood [27]: intramobility, extramobility, and transmobility. These classifications determine whether all or part of the mechanism will enter or exit the reference surface when actuated from its conformed position. This is particularly useful when designing a mechanism that must conform to the inside or outside of a rigid developable surface and would be unable to cross the surface.

Greenwood presents two graphical methods to determine the classification of a regular cylindrical mechanism: the Instant Center Reference Line (ICRL) method and the shadow method. The ICRL method determines the classification of a mechanism using the instant centers of each link. For a link *i*, the instant center with respect to ground is IC_{1i}. The ICRL is the line drawn through IC_{1i} and the center of the cylindrical cross section. The location of a link with respect to the ICRL determines whether or not the

mechanism is intramobile, extramobile, and/or transmobile. The green cou

Figure 4: A four-bar mechanism on a circle with the ICRL method illustrated for the coupler link.

Figure 5: The shadow method shown for a four-bar mechanism. As the center of the circle is contained within the shaded portion, the mechanism is exclusively transmobile.

pler link in Fig. 4 lies on either side of the ICRL. Therefore, the mechanism is exclusively transmobile, meaning that part of the mechanism will enter the cylinder while another part will exit.

The shadow method is limited to 1 DOF mechanisms with at least one

grounded four-bar loop. While faster than the ICRL method, the shadow method can only indicate the possibility of intramobility or extramobility. When the mechanism is represented with a skeleton diagram, the area between the input and output links is shaded, and the location of the center point of the circle relative to this shaded area can determine the possible classifications. An example of the shadow method is shown in Fig. 5. The center of the circle is inside the shaded region, meaning the mechanism is exclusively transmobile. A full description of the different cases for both the

ICRL and shadow method can be found in [27]. This paper extends these two methods to right conical developable mechanisms.

3. Conical Developable Mechanisms

As noted, a conical surface has ruling lines that converge to a point. A spherical mechanism can be mapped to a conical surface by placing the center of the reference sphere at the convergence point and aligning the joint axes to the ruling lines. Then, to satisfy the link-shape condition, the shape of the links are modified to conform to the surface. This process was outlined by Nelson et al. [1], and is shown in Fig. 6 mapping the mechanism from Fig. 2 to a conical surface. A method for analyzing developable mechanisms on a right circular conical surface is presented below.

While any spherical mechanism can be mapped to an arbitrary conical surface, there are some spherical mechanisms that can not be mapped to a regular right cone. Because a right cone only exists in one hemisphere of a reference sphere, to map a spherical mechanism to a right conical surface, it must have a configuration in which all link angles lie on one side of a reference sphere. The parameter T_4 defined in Eq. 4 can identify whether a four-bar mechanism with link angles α, η, β, and γ is contained within one hemisphere of the sphere or whether it wraps around the sphere [13]. The condition for this behavior is

$$\textit{mechanism}: \begin{cases} \text{hemisphere} & T_4 < 0 \\ \text{wraps around sphere} & T_4 > 0 \end{cases} \text{one}$$

With the properties outlined by Chiang [12] to simplify a spherical mechanism to minimal link angles, many mechanisms can be assembled with supplementary linkages to achieve the same motion with different link angles.

(a) (b)

(c)

Figure 6: (a) A four-bar spherical mechanism that is (b) mapped onto a conical surface with modified link shapes to conform to the surface and (c) shown in hardware.

If a supplementary linkage lies in one hemisphere, that mechanism can be mapped onto a right cylinder.

3.1. Projected Angles

Right circular cones can be defined by the rotation of a line at an angle about an axis, and here we define a developable mechanism on a cone by similar parameters. A reference frame F_0 is placed at the apex of the cone with the *y*-axis directed away from the cone along the center axis. The *z*-axis is then aligned in the direction of the first joint axis projected onto a plane perpendicular to the center axis through the apex as seen in Fig. 7. This will facilitate the description of the motion of a developable mechanism with respect to the geometry of the reference surface. Because the distance from the apex of the cone does not change the angle between the ruling lines, the location of the link along the surface does not change the behavior of the mechanism. The mechanism shown in Fig. 8 is the same as the mechanism shown in Fig. 6. The joint axes can be projected

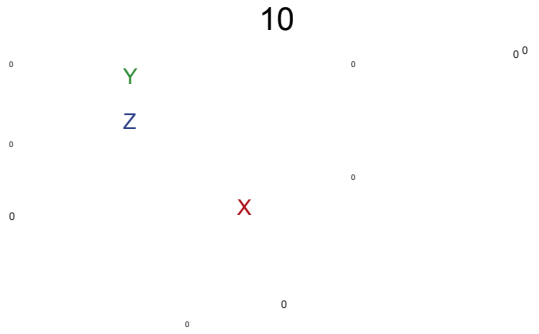

Figure 7: The global reference frame at the apex of the cone along with the projected angles on the *xz*-plane

Figure 8: The location of the link along the ruling line does not change the behavior of the mechanism, thus the two mechanisms exhibit the same relative motion between

joints.

onto the *xz* plane of frame F_0. The angles between the projected lines are referred to as *projected angles*. The signs of these angles follow the right-hand rule about the y-axis of frame F_0. While a physical link may extend beyond the joint axis, only the angles between the axes determine the kinematic behavior. Therefore, the projected angles are the minimum angle between the projected axes. This ensures that the magnitude of the projected angles will always be greater than 0 and less than or equal to 180°. The relationship 11

between a spherical link angle φ and the projected angle φ_0 is

$$cos\varphi = sin^2(\lambda) + cos^2(\lambda)cos\varphi_0 \quad (5)$$

for $0 \leq \lambda < 90°$, where λ is the cone angle measured from the *xz* plane to the surface of the cone.

When the value of λ is equal to zero, the cone can be represented by a two dimensional plane. In this case, the projected angles will be equal to the spherical link angles. When λ is equal to 90°, the cone will be a cylinder with an apex at infinity, and Eq. 5 should not be used. In its conformed position, the projected angles remain constant for any cross-section along the cone-axis.

For any n-bar spherical mechanism, the sum of the projected angles will always equal a multiple of 360°, or

$$(\varphi_1)_0 + (\varphi_2)_0 + ... + (\varphi_n)_0 = 360k \quad (6)$$

where *k* is an integer.

While the spherical link angle is always positive, when solving for the projected angle, the arccosine function can yield a positive or negative value indicating a positive or negative rotation about the y-axis. With the addi tional constraint of Eq. 6, the correct set of projected angles can be calculated

from the angles of a spherical mechanism. It is important to note that this method to calculate the projected angles only applies to the mechanism in its conformed position. Through the motion of the mechanism, these projected angles will change.

Projected angles can help determine whether a mechanism is in a con figuration with an open or crossed circuit. If a quadrilateral is formed by connecting the points that the projected angles intersect the unit circle in the proper order, either a convex or crossed quadrilateral will be formed. A convex quadrilateral corresponds to an open circuit, and the crossed quadri lateral to a crossed circuit. Because the projected angles have been defined to be between −180° and 180°

, and non-zero, they can be used to determine whether a conical developable mechanism in its conformed position is in its open or crossed configuration. Table 1 shows the conditions for each case. The projected angles for a spherical four-bar mechanism in its conformed

position are α_0, η_0, β_0, and γ_0.

These properties of projected angles allow for a reduction of the parameters needed to completely define a conical mechanism in its conformed position. A traditional spherical four-bar mechanism requires six parameters to

Table 1: Determination of the circuit configuration based on the projected angles.

	Product Sum	Circuit
$\alpha_0\eta_0\beta_0\gamma_0 > 0$	$\alpha_0 + \eta_0 + \beta_0 + \gamma_0 = 0$	*Open*
	$\alpha_0 + \eta_0 + \beta_0 + \gamma_0 \neq 0$	*Crossed*
$\alpha_0\eta_0\beta_0\gamma_0 < 0$	$\alpha_0 + \eta_0 + \beta_0 + \gamma_0 = 0$	*Crossed*
	$\alpha_0 + \eta_0 + \beta_0 + \gamma_0 \neq 0$	*Open*

define its position: α, η, β, and γ, the input angle θ, and the configuration. However, by constraining the mechanism to a conical surface, the conformed position can be defined by just four parameters: the cone angle λ, and three of the four projected angles (α_0, η_0, β_0, and γ_0).

These projected angles in the conformed position allow for connections to be made to analysis methods for developable mechanisms on a cylindrical surface, along with position analysis of the conical mechanism.

4. Intramobility, Extramobility, and Transmobility of Right Conical Developable Mechanisms

To determine whether a conical developable mechanism is intramobile, extramobile, and/or transmobile, the ICRL method and shadow method can be applied. The projections of the spherical links onto a cross-section of the reference cone along the cone axis resemble a cylindrical developable mechanism with link angles equal to the projected angles (Fig. 9a). As defined in [27], the ICRL method considers the motion of a link relative to its instant center in the conformed position of the mechanism. The spherical mechanism analog of the instant center is the instant pole axis. The projection of the instant pole axis of any spherical link onto the cross-section passes through the center of the circle and the instant center of the planar mechanism defined by the projected angles—the definition of the ICRL. The projected velocity vectors of the spherical mechanism onto the cross-section also coincide with the directions of the motion of the planar mechanism. Therefore, the conical mechanism will have the same classification as the cylindrical mechanism defined by the projected angles. This shows that both the ICRL and shadow methods can be used to classify right conical developable mechanisms. Figure 9 shows how both methods can be used for the coupler link of a conical mechanism.

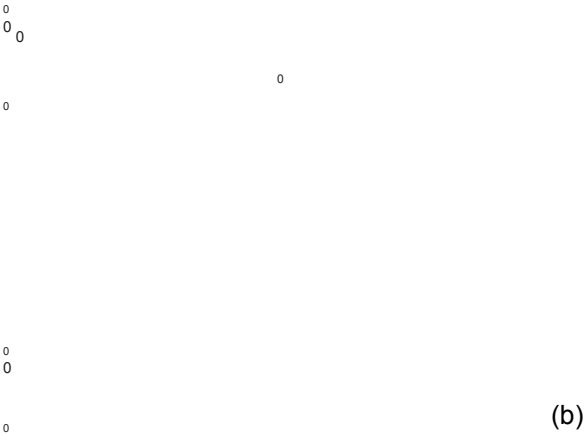

(b)

(a)

ICRL13

P

(c) (d)

Figure 9: (a) The planar projection of the mechanism with the instant pole axis of the coupler link with respect to ground and (b) the ICRL of its planar counterpart. Note that the line $ICRL_{13}$ is the planar projection of the instant pole axis $P_{\eta\gamma}$. (c) The shadow method is applied to the skeleton diagram of the planar mechanism created by the projected angles. (d) Based on both methods, the mechanism is exclusively transmobile as seen in the actuated position.

It is important to note that while the analysis is done in two dimensions, a conical mechanism will have three dimensional motion. An extramobile mechanism will also have a positive displacement in the *y*-direction, and an intramobile mechanism will have a negative displacement in the *y*-direction. A transmobile mechanism will have both positive and negative displacement in the *y*-direction.

5. Loop Sum Method to Find Cone Angle

This section introduces the Loop Sum Method as an approach to find the cone angle of a right conical reference surface to which a spherical mechanism can conform. The Loop Sum Method uses the properties of projected angles presented in Eq. 5 and 6.

If Eq. 5 is solved for the projected angle, the expression is

$$\varphi_0 = \pm \arccos \frac{\cos\varphi - \sin^2(\lambda)}{\cos^2(\lambda)} \qquad (7)$$

For an *n*-bar loop in a spherical mechanism, solving Eq. 7 for each link and adding them together generates a set of up to 2^n combinations due to the positive or negative solutions. Then, using a numerical or graphical approach, the cone angles which satisfy Eq. 6 can be found.

295 This approach is demonstrated with a spherical four-bar mechanism with link angles α, η, β,and γ. The projected angles from Eq. 7 are

$$\alpha_0 = \pm arccos\left(\frac{cos\alpha - sin^2(\lambda)}{cos^2(\lambda)}\right) \quad (8)$$

$$\eta_0 = \pm arccos\beta_0 = \pm arccos\left(\frac{cos\beta - sin^2(\lambda)}{cos^2(\lambda)}\right) \quad (9)$$

$$\pm arccos\gamma_0 = \pm arccos\left(\frac{cos\gamma - sin^2(\lambda)}{cos^2(\lambda)}\right) \quad (10)$$

$$\pm arccos\left(\frac{cos\eta - sin^2(\lambda)}{cos^2(\lambda)}\right) \quad (11)$$

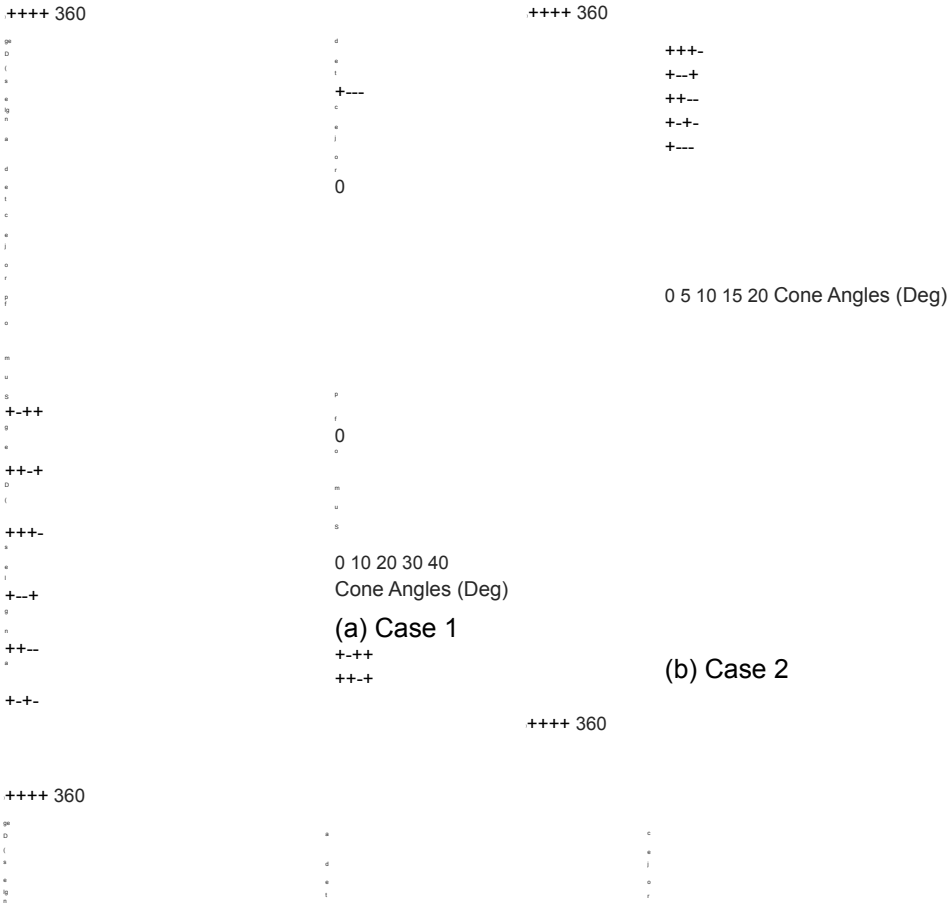

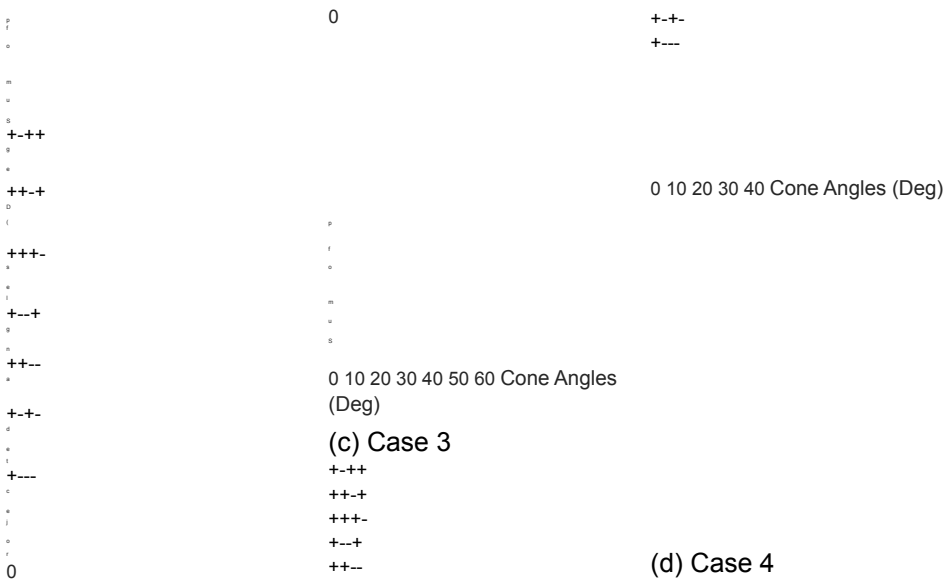

(c) Case 3

(d) Case 4

Figure 10: Eight of the sets of combinations of the Loop Sum Method. The legend indicates the signs of the projected angles in Eq. 12. The link angles used in the cases are (a) $\alpha = 120^\circ$, $\eta = 95^\circ$, $\beta = 45^\circ$, $\gamma = 85^\circ$, (b) $\alpha = 155^\circ$, $\eta = 50^\circ$, $\beta = 65^\circ$, $\gamma = 80^\circ$, (c) $\alpha = 100^\circ$, $\eta = 70^\circ$, $\beta = 90^\circ$, $\gamma = 60^\circ$. (d) $\alpha = 120^\circ$, $\eta = 50^\circ$, $\beta = 120^\circ$, $\gamma = 50^\circ$.

Substituting these projected angles into Eq. 6 gives

$$\pm\alpha_0 \pm \eta_0 \pm \beta_0 \pm \gamma_0 = 360k \quad (12)$$

The left hand side has a total of 16 possible combinations. However, eight of the sets are opposite of one another. For the following solutions, only the 300 combinations with a positive α_0 will be considered. By graphing the real solutions of these sums as functions of the cone angle λ, a solution is found where the sum is equal to a multiple of 360. Depending on the mechanism

classification, there are four possible solution cases as seen in Fig. 10(a-d). Each graph shows eight of the sums for each case. The first case of a Grashof 305 linkage will have two possible cone angles. The second case of a nonGrashof linkage will have only one possible cone angle. The third case of a folding mechanism will have up to one possible non-zero cone angle and one cone angle of zero. The final solution case of a mechanism with two sets of equal link angles will have infinite possibilities of cone angles.

310 This method will work for any mechanism which lies on one half of a reference sphere. If a mechanism wraps around the sphere as described in section 3, a supplementary linkage can be used to achieve the same motion. This supplementary linkage can then be used with this approach.

6. Position Analysis with Axis-Angle Rotations

315 In both planar and spherical mechanism analysis, when solving for the output angle as a function of the input angle, there are several possible solu tions based on the configuration of the mechanism. However, by

constraining the mechanism to a developable surface, a unique solution can be found analytically. When a spherical mechanism with link angles (φ_1, φ_2, ... , φ_n) is mapped to a conical surface, the dihedral angle between any two adjacent links in the conformed position $\theta_{n-1,n}$ can be calculated with the cone angle and the projected angles. To follow the convention set by McCarthy [13], the dihedral angle is measured from the plane created by link $n-1$ rotated about the joint axis shared with link n following the right-hand rule. For example, the input angle of a spherical four-bar θ as seen in Fig. 2 could be expressed as $\theta_{\gamma,\alpha}$ with this notation. The output angle ψ could be expressed as ($180^\circ - \theta_{\gamma,\beta}$). Using the spherical law of cosines [12] along with Eq. 5, the equations for these angles are

$$cos(m_\theta \theta_{n-1,n}) = cos\varepsilon - cos\varphi_{n-1} cos\varphi_n \\ sin\varphi_{n-1} sin\varphi_n \quad (13)$$

where

$$cos\varepsilon = sin^2\lambda + cos^2\lambda cos((\varphi_{n-1})_0 + (\varphi_n)_0) \quad (14)$$

The parameter m_θ can be 1 or -1 depending on the signs of $(\varphi_{n-1})_0$ and $(\varphi_n)_0$. Table 2 gives the value of m given the projected angles. Position analysis of spherical mechanisms is typically done using a sequence of rotations using the link angles [12]. By using axis-angle represen

Table 2: Values of m as a function of $(\varphi_{n-1})_0$ and $(\varphi_n)_0$

Sign of $(\varphi_{n-1})_0$	Value of $(\varphi_n)_0$	m_θ
$(\varphi_{n-1})_0 > 0$	$-1 < (\varphi_n)_0 < 0$	1
	all other cases	−1
$(\varphi_{n-1})_0 < 0$	$-1 < (\varphi_n)_0 < 0$	−1
	all other cases	1

tations of rotations, a different approach can describe the mechanism mo tion using only the projected angles and the geometry of the reference cone. Both analysis methods can yield the same results as long as the reference frames are established correctly, but the method presented in this section uses the projected angles of the mechanism rather than the link angles. Axis angle rotations can describe any composition of rotations by defining a single axis about which an object rotates a certain angle. This is based on Euler's theorem of a three-dimensional rotation [32]. The Rodrigues equation [33] describing the rotation of a vector v an angle θ about a unit vector $\hat{e}$ is

$v^0 = cos\theta\, v + sin\theta(\hat{e} \times v) + (1 - cos\theta)(v \cdot \hat{e})\hat{e}$ (15) In this paper, the rotation described by Eq. 15 will have the notation

$$v^0 = R_{e,\theta\hat{}}\, v \quad (16)$$

where $\hat{e}$ is the unit vector about which the vector v is rotated by θ. A cone can be considered as the rotation of a line segment about a center axis (cone axis). This axis-angle approach provides a way to visualize the sequence of rotations as rotations along a conical surface. By defining a reference frame as described in section 3.1, the first joint axis can be found by a rotation of λ about the x-axis. In its conformed position, every joint axis can then be identified by rotating the first joint axis about the y-axis (cone axis) using the projected angles. This approach is useful to describe the position of the mechanism with respect to the geometry of the reference cone.

Because of the link-shape condition, each link of a conical developable mechanism is a segment of a conical surface each with a unique cone axis. In the conformed position all of the axes are collinear, but as the mechanism moves, these cone axes shift relative to the reference cone. All of these shifts

can be described using a series of axis-angle rotations. The positions of any point along each link can then be determined. In this paper, this analysis method is presented for a four-bar conical developable mechanism.

Given a four-bar conical developable mechanism with projected angles (α_0, η_0, β_0, and γ_0) and a cone angle λ, the following equations describe the position of the joint axes (O, A, B, and C) with respect to the reference frame as described in section 3.1. The changes in the coupler and output angles as functions of the input angle can be calculated through methods presented in other work [12, 13].

1. Joint axis O is found by rotating the z-axis of the reference frame about the x-axis by λ.

$$O = R_{\hat{},\lambda}\,\hat{k} = \begin{bmatrix} 0 \\ -sin\lambda \\ cos\lambda \end{bmatrix} \quad (17)$$

2. The α-cone axis $\hat{e}_\alpha$ is found be rotating the y-axis about vector O by $\Delta\theta$ (change from the conformed position).

$$\hat{e}_\alpha = R_{O,\Delta\theta}\,\hat{j} \quad (18)$$

3. Joint axis A is found by rotating vector O about $\hat{e}_\alpha$ by α_0.

$$A = R_{e\hat{}_\alpha,\alpha_0} O \quad (19)$$

4. The η-cone axis $\hat{}e_\eta$ is found by rotating $\hat{}e_\alpha$ about A by $\Delta\xi$ (change in the coupler angle from conformed position).

$$e\hat{}_\eta = R_{A,\Delta\xi} e\hat{}_\alpha \quad (20)$$

5. The joint axis B is found by rotating vector A about $\hat{}e_\eta$ by η_0.

$$B = R_{e\hat{}_\eta,\eta_0} A \quad (21)$$

6. The joint axis C is found by rotating vector O about the y-axis by γ_0.

$$C = R\hat{}_{j,\gamma_0} O \quad (22)$$

7. An alternate equation for joint axis B is found by rotating vector C about $\hat{}e_\beta$ by β_0.

$$B = R_{e\hat{}_\beta,\beta_0} C \quad (23)$$

where

$$e\hat{}_\beta = R_{C,\Delta\psi} \hat{j} \quad (24)$$

These equations are used to find just the location of the joint axis. A link may extend beyond the joint axis along the surface of the cone. To find any point along a link, Eqs. 19, 21, and 23 can be used with different angles to find the position of a point along the α, η, and β links, respectively. The same approach can be extended to mechanisms with more links.

7. Multiloop Conical Developable Mechanisms

Some multiloop spherical mechanisms can also be mapped onto a regular conical surface provided that all of their joint axes align with the ruling lines of a reference conical surface. The methods for analysis presented in this paper can also be applied to multiloop linkages.

7.1. Loop Sum Method for Multiloop Mechanisms

A multiloop linkage is constructed from several connected loops to create a single degree of freedom mechanism. As the Loop Sum Method described in section 5 determines the possible cone angles for a single loop mechanism, it would need to be applied to each individual loop of a multiloop mechanism and yield the same cone angle each time to map the mechanism to a right conical surface. For example, a six-bar linkage typically contains two closed loops (two four-bar loops in a Watt linkage, and a four-bar and five-bar loop in a Stephenson linkage). When the Loop Sum Method is

applied to each loop, the mechanism can only be mapped to a conical surface if a common cone angle is found. This is an important distinction as any spherical four-bar mechanism can be mapped to a cone, but few spherical multiloop mechanisms can. Therefore, the Loop Sum Method defines a design requirement for multiloop mechanisms rather than a tool to be applied on an arbitrary mechanism. An example of a spherical Stephenson 2 linkage mapped to a cone is shown in Fig. 11.

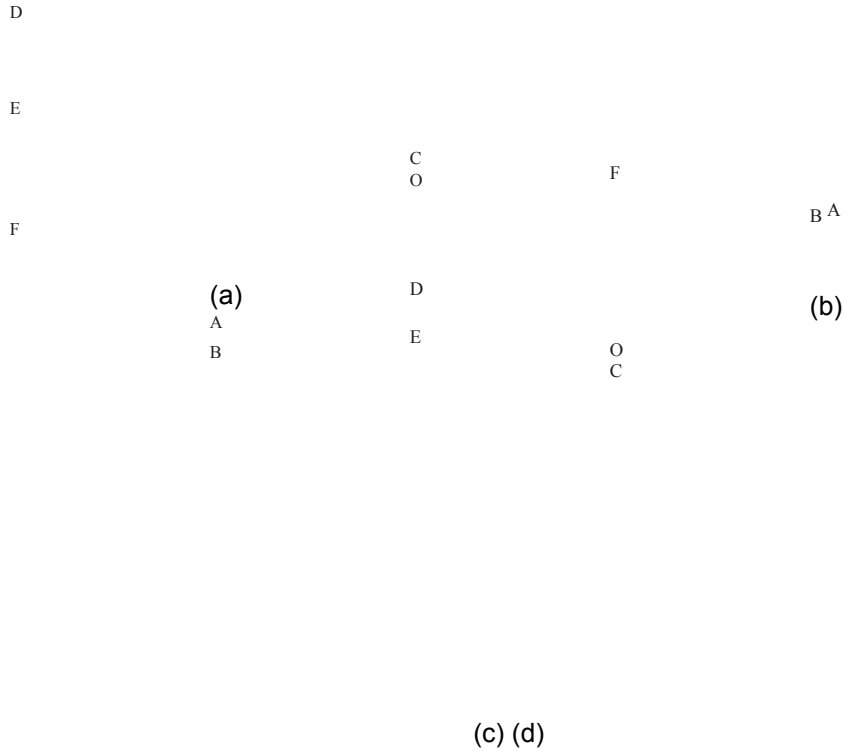

Figure 11: (a) A spherical Stephenson 2 linkage (b) mapped onto a regular conical surface. (c) Hardware demonstrates the mechanism in the conformed and (d) actuated positions. The displayed mechanism has a cone angle of 20° and projected angles of $(\varphi_{OA})_0 = -40^\circ$, $(\varphi_{AB})_0 = -20^\circ$, $(\varphi_{BC})_0 = -45^\circ$, $(\varphi_{CD})_0 = -68^\circ$, $(\varphi_{DE})_0 = 28^\circ$, $(\varphi_{EF})_0 = 30^\circ$.

7.2. Position analysis of Multiloop Mechanisms

The method of using axis-angle rotations to analyze the position of a mechanisms with respect to the apex of the cone can be applied to multiloop mechanisms. As with four-bar mechanisms, each link represents a segment of the cone with a distinct cone axis. Through a sequence of axis-angle rotations, the position along each link can be found provided that the changes in dihedral angles from the conformed position are known.

8. Conclusion

This paper has presented several definitions and approaches to aid in the design and analysis of conical developable mechanisms. By conforming to a conical surface, a spherical mechanism can achieve complex three dimensional

motion while stowing compactly to a designated configuration. The projected angles of the joint axes allow for a reduction of the parameters needed to completely define a mechanism. These angles also facilitate the adaptation of other analysis methods for planar mechanisms on cylindrical surfaces.

This paper introduces several methods to design conical developable mechanisms. With the properties of projected angles, the cone angle of a right conical reference surface can be found for any traditional spherical four-bar mechanism. An alternate method for the position analysis of a four-bar mechanism was developed that uses rotations about the axis of the reference cone. This can determine the position of any point along the link throughout a mechanism's motion with respect to the reference cone surface. The princi ples presented can also be applied generally to mechanisms with more than four links.

Acknowledgements

This material is based on work supported by the National Science Foundation under NSF Grant No. 1663345.

References

[1] T. G. Nelson, T. K. Zimmerman, S. P. Magleby, R. J. Lang, L. L. Howell, Developable mechanisms on developable surfaces, Science Robotics 4 (27) (2019) eaau5171. doi:10.1126/scirobotics.aau5171.

[2] S. R. Woodruff, E. T. Filipov, Structural Analysis of Curved Folded Deployables, in: Earth and Space 2018, American Society of Civil Engineers, 2018, pp. 793–803. doi:10.1061/9780784481899.075.

[3] P. Bo, Y. Zheng, X. Jia, C. Zhang, Multi-strip smooth developable surfaces from sparse design curves, CAD Computer Aided Design 114 (2019) 1–12. doi:10.1016/j.cad.2019.05.001.

[4] K. Gavriil, A. Schiftner, H. Pottmann, Optimizing B-spline surfaces for developability and paneling architectural freeform surfaces, CAD Computer Aided Design 111 (2019) 29–43. doi:10.1016/j.cad.2019.01. 006.

[5] G. Glaeser, F. Gruber, Developable surfaces in contemporary architecture, Journal of Mathematics and the Arts 1 (1) (2007) 59–71. doi:10.1080/17513470701230004.

[6] J. J. Lim, A. G. Erdman, A review of mechanism used in

laparoscopic surgical instruments, Mechanism and Machine Theory 38 (11) (2003) 1133–1147. doi:10.1016/S0094-114X(03)00063-6.

[7] R. Jha, S. Bodhari, V. Sudhakar, P. Mahapatra, A surface modeling paradigm for electromagnetic applications in aerospace structures, in: Digest on Antennas and Propagation Society International Symposium, IEEE, 1989, pp. 227–230. doi:10.1109/APS.1989.134656.

[8] S. A. Zirbel, R. J. Lang, M. W. Thomson, D. A. Sigel, P. E. Walke meyer, B. P. Trease, S. P. Magleby, L. L. Howell, Accommodating Thickness in Origami-Based Deployable Arrays, Journal of Mechanical Design 135 (11) (nov 2013). doi:10.1115/1.4025372.

[9] M. Lum, J. Rosen, M. Sinanan, B. Hannaford, Optimization of a Spheri cal Mechanism for a Minimally Invasive Surgical Robot: Theoretical and Experimental Approaches, IEEE Transactions on Biomedical Engineering 53 (7) (2006) 1440–1445. doi:10.1109/TBME.2006.875716.

[10] G. Mullineux, Atlas of spherical four-bar mechanisms, Mechanism and Machine Theory 46 (11) (2011) 1811–1823. doi:10.1016/J. MECHMACHTHEORY.2011.06.001.

[11] D. Ruth, J. McCarthy, The design of spherical 4R linkages for four specified orientations, Mechanism and Machine Theory 34 (5) (1999) 677–692. doi:10.1016/S0094-114X(98)00048-2.

[12] C. Chiang, Spherical kinematics in contrast to planar kinematics, Mech anism and Machine Theory 27 (3) (1992) 243–250. doi:10.1016/ 0094-114X(92)90014-9.

[13] J. M. McCarthy, G. S. Soh, Geometric design of linkages, Springer, 2011.

[14] J. Chu, J. Sun, Numerical atlas method for path generation of spherical four-bar mechanism, Mechanism and Machine Theory 45 (6) (2010) 867– 879. doi:10.1016/J.MECHMACHTHEORY.2009.12.005.

[15] X. Li, P. Zhao, A. Purwar, Q. J. Ge, A unified approach to exact and approximate motion synthesis of spherical four-bar linkages via kine matic mapping, Journal of Mechanisms and Robotics 10 (1) (feb 2018). doi:10.1115/1.4038305.

[16] A. P. Murray, F. Pierrot, Design of a High-Speed Spherical Four-Bar Mechanism for Use in a Motion Common in Assembly Processes, in: Volume 8: 31st Mechanisms and Robotics Conference, Parts A and B, ASME, 2007, pp. 511–518. doi:10.1115/DETC2007-35354.

[17] S. W. Son, D. S. Kwon, A convex programming approach to the base placement of a 6-DOF articulated robot with a spherical wrist, Interna

tional Journal of Advanced Manufacturing Technology 102 (9-12) (2019) 3135–3150. doi:10.1007/s00170-019-03391-0.

[18] S. Bai, X. Li, J. Angeles, A review of spherical motion generation us ing either spherical parallel manipulators or spherical motors, Mech anism and Machine Theory 140 (2019) 377–388. doi:10.1016/j. mechmachtheory.2019.06.012.

[19] Z. Tao, Q. An, Interference analysis and workspace optimization of 3- RRR spherical parallel mechanism, Mechanism and Machine Theory 69 (2013) 62–72. doi:10.1016/J.MECHMACHTHEORY.2013.05.004.

[20] J. Sun, W. Liu, J. Chu, Synthesis of spherical four-bar linkage for open path generation using wavelet feature parameters, Mechanism and Machine Theory 128 (2018) 33–46. doi:10.1016/j.mechmachtheory. 2018.05.008.

[21] Y. Chen, W. Lv, R. Peng, G. Wei, Mobile assemblies of four-spherical 4R-integrated linkages and the associated four-crease-integrated rigid origami patterns, Mechanism and Machine Theory 142 (2019) 103613. doi:10.1016/j.mechmachtheory.2019.103613.

[22] M. N. Castro, J. Rasmussen, M. S. Andersen, S. Bai, A compact 3-DOF shoulder mechanism constructed with scissors linkages for exoskeleton applications, Mechanism and Machine Theory 132 (2019) 264–278. doi: 10.1016/J.MECHMACHTHEORY.2018.11.007.

[23] M. Sun, E. Fiume, A technique for constructing developable surfaces, in: Graphics Interface, Toronto, 1996, pp. 176–185. doi:10.20380/GI1996. 21.

[24] V. Ushakov, Developable surfaces in Euclidean space, Journal of the Australian Mathematical Society 66 (03) (1999) 388. doi:10.1017/ S1446788700036685.

[25] S. Lawrence, Developable Surfaces: Their History and Application, Nexus Network Journal 13 (3) (2011) 701–714. doi:10.1007/ s00004-011-0087-z.

[26] R. L. Norton, Design of Machinery: an introduction to the synthesis and analysis of mechanisms and machines, McGraw-Hill Professional, 2004.

[27] J. R. Greenwood, S. P. Magleby, L. L. Howell, Developable mechanisms on regular cylindrical surfaces, Mechanism and Machine Theory 142 (2019) 103584. doi:10.1016/J.MECHMACHTHEORY.2019.103584.

[28] H. Pottmann, J. Wallner, Computational line geometry, Springer, 2009.

[29] C. Chiang, On the classification of spherical four-bar linkages, Mechanism and Machine Theory 19 (3) (1984) 283–287. doi:10.1016/0094-114X(84)90061-2.

[30] A. Erdman, G. Sandor, Mechanism Design Analysis and Synthesis, 2nd Edition, Prentice Hall, 1991.

[31] S. Zarkandi, Isotropy analysis of spherical mechanisms using an instantaneous-pole based method, Engineering Science and Technol ogy, an International Journal 20 (1) (2017) 240–246. doi:10.1016/j.jestch.2016.08.016.

[32] B. Palais, R. Palais, S. Rodi, A Disorienting Look at Euler's Theorem on the Axis of a Rotation, American Mathematical Monthly 116 (10) (2009) 892–909. doi:10.4169/000298909X477014.

[33] B. Paul, On the Composition of Finite Rotations, The American Mathematical Monthly 70 (8) (1963) 859–862. doi:10.2307/2312674.

Conflict of Interest

Conflict of Interest and Authorship Conformation Form

Please check the following as appropriate:

- o All authors have participated in (a) conception and design, or analysis and interpretation of the data; (b) drafting the article or revising it critically for important intellectual content; and (c) approval of the final version.
- o This manuscript has not been submitted to, nor is under review at, another journal or other publishing venue.
- o The authors have no affiliation with any organization with a direct or indirect financial interest in the subject matter discussed in the manuscript